ELSEVIER

www.elsevier.nl/locate/jorganchem

Journal of Organometallic Chemistry 599 (2000) 221–231

Journal of Organometallic Chemistry

Reactions of cationic dirhodium and diiridium complexes [Cp*M(μ-Cl)(μ-SPr^i)$_2$MCp*][OTf] (M = Rh, Ir) with terminal alkynes. Comparison with the diruthenium system

Youichi Ishii, Ken-ichi Ogio, Masayuki Nishio, Mikael Retbøll, Shigeki Kuwata, Hiroyuki Matsuzaka [1], Masanobu Hidai *

Department of Chemistry and Biotechnology, Graduate School of Engineering, The University of Tokyo, Hongo, Bunkyo-ku, Tokyo 113-8656, Japan

Received 11 November 1999; received in revised form 24 December 1999; accepted 24 December 1999

Abstract

Reactions of the cationic dirhodium and diiridium complexes [Cp*M(μ-Cl)(μ-SPr^i)$_2$MCp*][OTf] (**2**, M = Rh; **3**, M = Ir; Cp* = η^5-C$_5$Me$_5$, OTf = OSO$_2$CF$_3$) with terminal alkynes were investigated. Treatment of **2** and **3** with methyl propiolate afforded the cationic complexes [Cp*MCl(μ-SPr^i){μ-S(Pr^i)C=CHCOOMe}MCp*][OTf] (**4**, M = Rh; **5**, M = Ir), in which the substituted vinyl ligand forms an M(1)–C–S–M(2) bridge and is further coordinated to the M(1) center at the carbonyl oxygen. On the other hand, [Cp*IrCl(μ-SPr^i){μ-C(SPr^i)=CH$_2$}IrCp*][OTf] (**8**), in which the olefinic C=C bond of the α-(isopropylthio)vinyl ligand also works as an η^2 ligand, was obtained by the reaction of **3** with acetylene gas. Complex **3** reacted with 1,1-diphenyl- or 1,1-ditolyl-2-propyn-1-ol to give the hydroxycarbene complexes [Cp*IrCl(μ-SPr^i)$_2$Ir{=C(OH)CH=CAr$_2$}Cp*][OTf](**11**) Ar = Ph; **12**, Ar = Tol), while the reactions of complexes **2** and **3** with 3-butyn-1-ol and 4-pentyn-1-ol produced cyclic alkoxycarbene complexes [Cp*MCl(μ-SPr^i)$_2$M{=C(CH$_2$)$_n$ + 2O}Cp*][OTf] (**15**, M = Rh, n = 1; **16**, M = Ir, n = 1; **17**, M = Ir, n = 2). All of the products are considered to be formed via the initial formation of a dinuclear vinylidene or allenylidene complex followed by the nucleophilic attack of an SPr^i ligand, H$_2$O molecule, or the ω-OH group at the C$_\alpha$ atom of the vinylidene-type ligand. The intermediate vinylidene and allenylidene species are regarded to have higher reactivity in the nucleophilic addition reactions than the corresponding diruthenium complexes, and the difference in the reactivities is interpreted in terms of the extended Hückel molecular orbital calculations of model complexes. The molecular structures of complexes **3**, **4**, **5**, [Cp*IrCl(μ-SPr^i){μ-C(SPr^i)=CH$_2$}IrCp*][PF$_6$]·THF (**8′**·THF), **12**, and **16** were determined by X-ray diffraction studies.

Keywords: Rhodium; Iridium; Dinuclear complex; Alkyne; Crystal structure; MO calculations

1. Introduction

Multinuclear transition-metal complexes are expected to promote unique transformations of substrate molecules that can hardly be attained at a monometallic coordination site [1]. In our previous studies on multinuclear complexes with bridging sulfur-based ligands, we have synthesized a series of thiolato-bridged dinuclear ruthenium complexes such as [Cp*RuCl(μ-SPr^i)$_2$RuClCp*], [Cp*Ru(μ-SPr^i)$_3$RuCp*], and [Cp*-RuCl(μ-SPr^i)$_2$Ru(OH$_2$)Cp*][OTf] (**1**) (Cp* = η^5-C$_5$Me$_5$, OTf = OSO$_2$CF$_3$), and have demonstrated that the dinuclear cores of these complexes provide robust and effective reaction sites for a variety of stoichiometric as well as catalytic transformations of organic substrates [2]. In particular, the cationic complex **1** shows high reactivities toward terminal alkynes [3–6]. Thus, facile coupling of phenylacetylene takes place to give the diruthenium complex with an indan-type framework [3], while ferrocenylacetylene is catalytically converted into the linear dimer and trimer [4]. Dinuclear vinylidene [5] and allenylidene [3] complexes relevant to these coupling reactions of alkynes have also been

* Corresponding author. Fax: +81-3-58417265.

[1] Present address: Department of Chemistry, Tokyo Metropolitan University, Minami-osawa, Tokyo 192-0397, Japan.

0022-328X/00/$ - see front matter
PII: S0022-328X(00)00002-4

synthesized. Furthermore, a related dinuclear complex [Cp*RuCl(μ-SMe)$_2$RuClCp*] has been found to work as an active catalyst for the stereoselective dimerization of a wide range of terminal alkynes [6].

Development of the rich chemistry of the thiolato-bridged diruthenium complexes stimulated us to extend our studies to the corresponding dirhodium and diiridium systems [7–9], which are expected to exhibit distinct reactivities from those of the diruthenium complexes owing to the difference in the numbers of their valence electrons. Now we have found that the cationic dirhodium and diiridium complexes [Cp*M(μ-Cl)(μ-SPr^i)$_2$MCp*][OTf] (**2**, M = Rh; **3**, M = Ir) readily react with terminal alkynes to give several types of products depending upon the substituents of the alkynes. Interestingly, most products obtained are not simple analogs of those formed from the cationic diruthenium complex **1**. The difference in the reaction courses observed with complexes **1** and **2** or **3** is interpreted in terms of the molecular orbital calculations of cationic dinuclear vinylidene model complexes.

2. Results and discussion

2.1. Molecular structure of complex 3

In a previous paper, we have reported that the cationic dirhodium and diiridium complexes **2** and **3** can be prepared by treatment of the dichloro complexes [Cp*MCl(μ-SPr^i)$_2$MClCp*] (M = Rh, Ir) with AgOTf and are subsequently converted into the cationic hydrido complexes [Cp*M(μ-H)(μ-SPr^i)$_2$-MCp*][OTf] [7]. However, solid-state structures of **2** and **3** have not been determined. Now we have undertaken an X-ray diffraction study of the diiridium complex **3**. As shown in Fig. 1, the dinuclear core of **3** is bridged by one chloro and two thiolato ligands, the

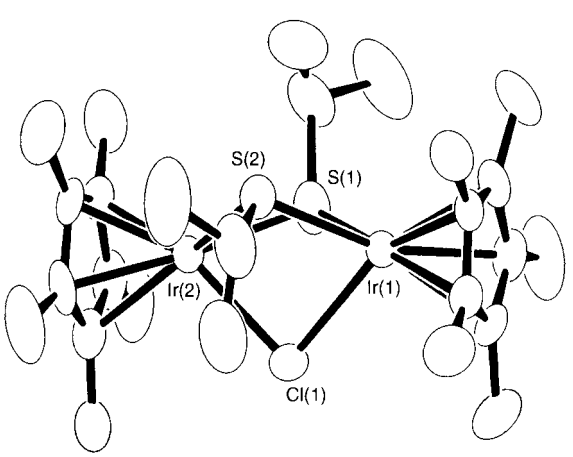

Fig. 1. Structure of the cationic part in **3**. Thermal ellipsoids are shown at the 50% probability level.

Table 1
Selected interatomic distances (Å) and angles (°) in **3**

Distances			
Ir(1)–Cl(1)	2.464(3)	Ir(1)–S(1)	2.413(3)
Ir(1)–S(2)	2.368(3)	Ir(2)–Cl(1)	2.462(3)
Ir(2)–S(1)	2.405(3)	Ir(2)–S(2)	2.384(3)
Ir(1)···Ir(2)	3.3436(8)		
Angles			
Cl(1)–Ir(1)–S(1)	73.3(1)	Cl(1)–Ir(1)–S(2)	80.42(9)
S(1)–Ir(1)–S(2)	78.1(1)	Cl(1)–Ir(2)–S(1)	73.4(1)
Cl(1)–Ir(2)–S(2)	80.18(10)	S(1)–Ir(2)–S(2)	77.94(10)
Ir(1)–Cl(1)–Ir(2)	85.49(8)	Ir(1)–S(1)–Ir(2)	87.91(9)
Ir(1)–S(2)–Ir(2)	89.44(9)		

latter of which takes an *anti* configuration. Thus, one of the Pr^i groups is placed at the axial position with respect to the Ir_2S_2 ring, while the other is at the equatorial position. The two Cp* ligands are located nearly parallel to each other (the dihedral angle between the two Cp* planes is 2.7°). Selected bond distances and angles are listed in Table 1. It should be noted that, unlike complex **3**, the related cationic diruthenium complexes **1** [3] and [Cp*RuCl(μ-SFc)$_2$RuCp*][OTf] (Fc = ferrocenyl) [10] have a doubly thiolato-bridged core with a terminally bound chloro ligand. Similar structural variation was also observed with the cationic hydrido complexes [Cp*MH(μ-SPr^i)$_2$MCp*][OTf] (M = Ru, Rh, Ir), where the diruthenium complex takes a doubly bridged structure with a terminal hydrido ligand, while the dirhodium and diiridium complexes have a triply bridged core with the hydrido ligand at the bridging position [7].

The ^{1}H-NMR spectrum of **3** in acetone-d_6 at room temperature showed one broad signal at δ 1.44 attributable to the Me resonance of the μ-SPr^i ligands [7], suggesting that the structure of **3** in solution is fluxional at room temperature At 0°C or below, the signal at δ 1.44 split into two doublets (δ 1.33 (J = 6.9 Hz), 1.40 (J = 6.9 Hz) at 0°C), which is in good agreement with the solid-state structure with the *anti* configuration. On the other hand, the signal changed into a doublet (δ 1.41 (J = 6.9 Hz)) on warming to 50°C. These observations are accounted for by considering the facile interconversion of the arrangement of the SPr^i groups at 50°C (Eq. (1)). The ^{1}H-NMR spectrum of **2** in acetone-d_6 exhibited similar temperature dependence. At room temperature the Me signals of the μ-SPr^i ligands appeared as two broad doublets (δ 1.38 (J = 6.9 Hz), 1.49 (J = 6.9 Hz)), which changed into a very broad signal (δ 1.5) and sharp doublets at 50 and 0°C, respectively. Judging from the NMR behavior, we conclude that complex **2** also has a triply bridged structure analogous to that of **3** in the solid state, and the stereochemistry of the SPr^i groups is fluxional in solution.

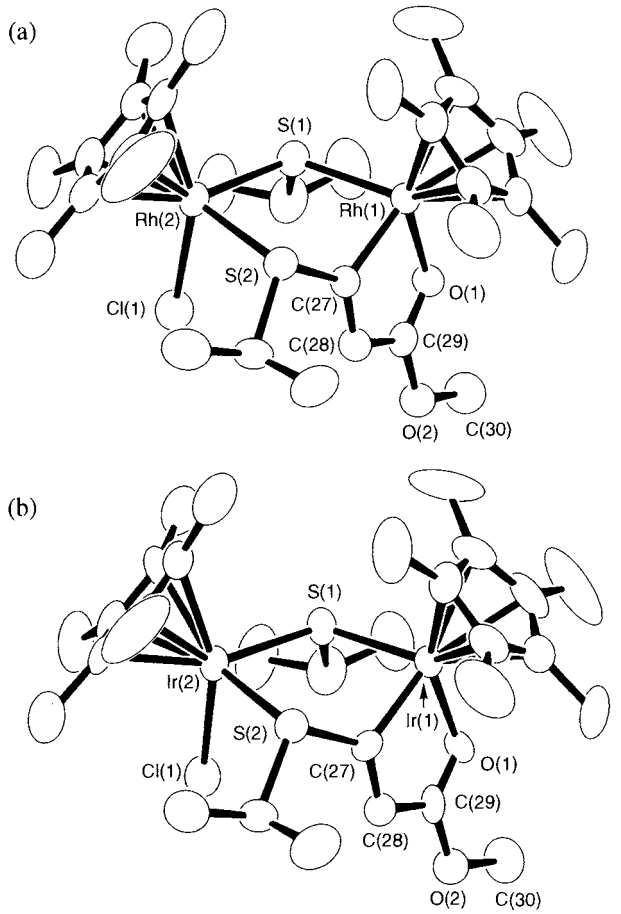

Fig. 2. Structures of the cationic parts in **4** (a) and **5** (b). Thermal ellipsoids are shown at the 50% probability level.

Table 2
Selected interatomic distances (Å) and angles (°) in **4** and **5**

	4 (M = Rh)	**5** (M = Ir)
Distances		
M(1)–S(1)	2.366(2)	2.363(2)
M(1)–O(1)	2.167(3)	2.159(6)
M(1)–C(27)	2.010(5)	1.994(10)
M(2)–Cl(1)	2.386(1)	2.389(2)
M(2)–S(1)	2.422(2)	2.409(3)
M(2)–S(2)	2.450(2)	2.423(2)
O(1)–C(29)	1.256(6)	1.23(1)
C(27)–C(28)	1.335(6)	1.32(1)
C(28)–C(29)	1.438(7)	1.42(1)
M(1)···M(2)	3.9713(6)	3.9565(6)
Angles		
S(1)–M(1)–O(1)	99.0(1)	97.2(2)
S(1)–M(1)–C(27)	82.8(1)	83.0(2)
O(1)–M(1)–C(27)	78.0(2)	75.9(3)
S(1)–M(2)–S(2)	87.37(5)	87.78(9)
M(2)–S(2)–C(27)	99.0(2)	100.0(3)
M(1)–O(1)–C(29)	108.9(3)	110.5(6)
M(1)–C(27)–S(2)	117.4(3)	116.0(4)
M(1)–C(27)–C(28)	116.6(4)	119.1(8)
S(2)–C(27)–C(28)	125.9(4)	124.6(8)
C(27)–C(28)–C(29)	112.7(5)	110.8(9)
O(1)–C(29)–C(28)	122.3(5)	122.4(9)

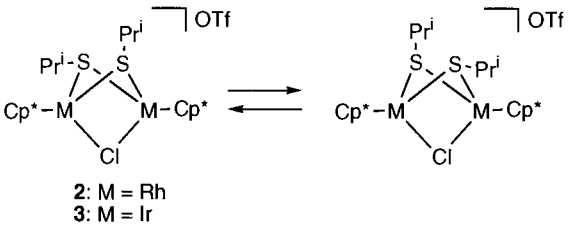

(1)

2.2. Reactions of complexes 2 and 3 with alkynes

Complexes **2** and **3** were found to react with terminal alkynes to give a series of dinuclear complexes in which the alkyne molecule is incorporated as a vinyl or carbene ligand. When **2** and **3** were allowed to react with methyl propiolate at room temperature, the cationic α-(isopropylthio)vinyl complexes [Cp*MCl(μ-SPr^i){μ-S(Pr^i)C=CHCOOMe}MCp*][OTf] (**4**, M = Rh; **5**, M = Ir), formed by the coupling of one SPr^i ligand and methyl propiolate, were isolated as orange or orange–red crystals in good yield (Eq. (2)). In the ^{1}H-NMR spectra, complexes **4** and **5** showed the vinyl signal as a singlet (**4**, δ 6.18; **5**, δ 7.15) in addition to the Cp*, Pr^i, and COOMe signals. The IR spectra exhibited a strong absorption at 1572 cm^{-1} for **4** and 1559 cm^{-1} for **5**, which are assigned to the ν(CO) of a coordinated COOMe group. These spectral features are in full accordance with the formulation.

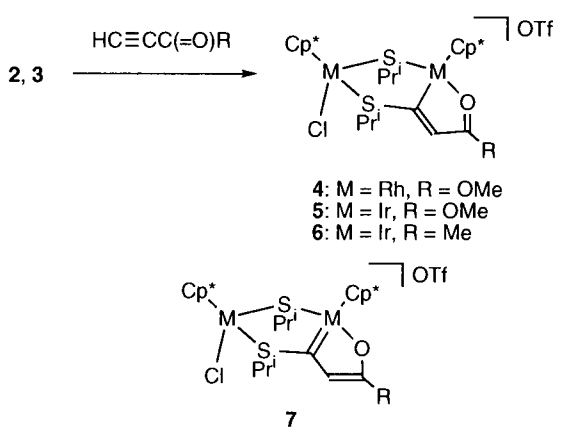

(2)

The reactions of **2** and **3** with methyl propiolate in acetone-d_6 were followed by ^{1}H-NMR. It was revealed that the conversion of the iridium complex **3** to **5** was completed within a few minutes, while the reaction of the rhodium complex **2** was much slower and required several hours to go completion. In both cases, no intermediate was observed. Treatment of complex **3** with 3-butyn-2-one also afforded an analogous complex [Cp*IrCl(μ-SPr^i){μ-S(Pr^i)C=CHCOMe}IrCp*][OTf] (**6**).

The molecular structures of **4** and **5** were confirmed by X-ray diffraction analysis. ORTEP drawings of the cationic parts in **4** and **5** are illustrated in Fig. 2, and selected bond distances and angles are contained in Table 2. The structures of these complexes are closely

related to each other. It has unambiguously been demonstrated that one of the SPr^i ligands in **2** and **3** and a methyl propiolate molecule are coupled to construct a bridging $C(SPr^i)$=CHCOOMe ligand, whose carbonyl oxygen is further coordinated to the M(1) atom to form a metallacycle. In each complex, the M(1), C(27), C(28), C(29), and O(1) atoms in the metallacycle are essentially coplanar. The Rh(1)–C(27) and Ir(1)–C(27) distances at 2.010(5) and 1.994(10) Å, respectively, are shorter than common Rh–C(vinyl) and Ir–C(vinyl) bonds (2.04–2.07 Å) [11,12], indicating some contribution of the carbene–enolato structure **7** [12,13]. In contrast to complexes **2** and **3**, complexes **4** and **5** adopt a *syn* configuration with respect to the SPr^i ligands. The M(1)–S(1)–M(2)–S(2)–C(27) cycle takes an envelop conformation, where the M_2S_2 moiety is almost planar.

On the other hand, a different type of α-(isopropylthio)vinyl complex was obtained from the reaction of **3** with acetylene gas. Thus, treatment of an acetone solution of **3** with acetylene gas caused rapid color change from orange to purple, and complex [Cp*IrCl(μ-SPr^i){μ-$C(SPr^i)$=CH_2}IrCp*][OTf] (**8**) was isolated in good yield (Eq. (3)). Complex **8** showed two doublet signals assignable to the vinyl protons at δ 3.41 ($J = 3.5$ Hz) and 4.47 ($J = 3.5$ Hz) in the ^{1}H-NMR spectrum, and the elemental analysis data were consistent with the incorporation of one acetylene molecule into complex **3**. However, chemical shifts of the vinyl protons are significantly different from those observed with complexes **4**–**6**, suggesting a variance in the coordination mode of the vinyl ligand.

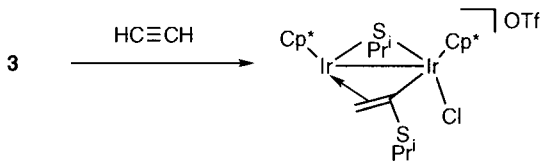

(3)

8

The structure of the dinuclear cation in **8** was fully established by X-ray analysis of the corresponding $[PF_6]^-$ salt [Cp*IrCl(μ-SPr^i){μ-$C(SPr^i)$=CH_2}IrCp*]-[PF_6]·THF (**8′**·THF). An ORTEP view is given in Fig. 3, and important bond distances and angles are in Table 3. Complex **8′** contains a $C(SPr^i)$=CH_2 ligand σ-bonded to the Ir(2) atom, and the olefinic part of this ligand is further coordinated to the Ir(1) atom, while the SPr^i group has no interaction with the metal centers. The Ir(1)–Ir(2) contact at 2.8011(7) Å corresponds to an Ir–Ir single bond [14], which is in harmony with the 34 e^- core of this cation.

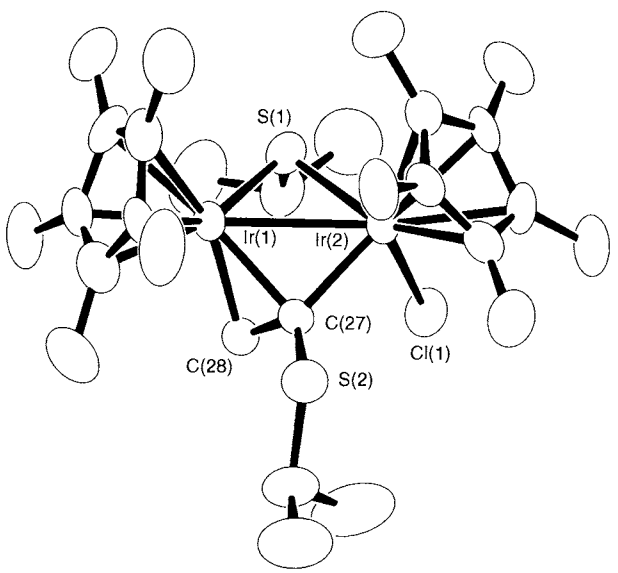

Fig. 3. Structure of the cationic part in **8′**·THF. Thermal ellipsoids are shown at the 50% probability level.

Table 3
Selected interatomic distances (Å) and angles (°) in **8′**·THF

Distances			
Ir(1)–Ir(2)	2.8011(7)	Ir(1)–S(1)	2.307(3)
Ir(1)–C(27)	2.10(1)	Ir(1)–C(28)	2.16(1)
Ir(2)–Cl(1)	2.390(3)	Ir(2)–S(1)	2.359(3)
Ir(1)–C(27)	2.08(1)	S(2)–C(27)	1.73(1)
C(27)–C(28)	1.43(1)		
Angles			
S(1)–Ir(1)–C(27)	92.0(3)	S(1)–Ir(1)–C(28)	88.6(3)
C(27)–Ir(1)–C(28)	39.1(4)	Cl(1)–Ir(2)–S(1)	93.1(1)
Cl(1)–Ir(2)–C(27)	84.6(3)	S(1)–Ir(2)–C(27)	91.2(3)
Ir(1)–C(27)–Ir(2)	84.2(4)	Ir(1)–C(27)–S(2)	123.0(6)
Ir(1)–C(27)–C(28)	72.4(6)	Ir(2)–C(27)–S(2)	121.6(6)
Ir(2)–C(27)–C(28)	115.8(8)	S(2)–C(27)–C(28)	121.4(8)
Ir(1)–C(28)–C(27)	123.0(6)		

The reaction of **2** with acetylene gas was also investigated, and a complex that exhibited two vinyl signals in the ^{1}H-NMR spectrum (δ 5.81(s), 6.22 (d, $J = 1.3$ Hz)) was obtained. We consider that a dirhodium complex with a $C(SPr^i)$=CH_2 ligand was also formed in this reaction, but unfortunately the accurate structure of this species still remains unclarified.

Considerable attention has recently been paid to the rearrangement of terminal alkynes to vinylidene ligands on complexation to a metal fragment and the electrophilic reactivities of the C_α atom of the vinylidene ligands thus formed [15]. In the above transformations, complexes **4**–**6** and **8** are considered to be formed via the dinuclear vinylidene intermediates **9** generated by the reactions of **2** or **3** with alkynes (Scheme 1). When methyl propiolate or 3-butyn-2-one is used as the alkyne, intramolecular attack by one of the SPr^i ligands onto the C_α atom of the vinylidene ligand in **9** followed by coordination of the C=O group leads to the formation of complexes **4**–**6**. Related nucleophilic migration of a coordinated amine [16] or H_2O [17] onto the C_α atom of a vinylidene ligand has been described in literature. For the reaction of **3** with acetylene gas, the vinylidene–SPr^i coupling followed by the migration of

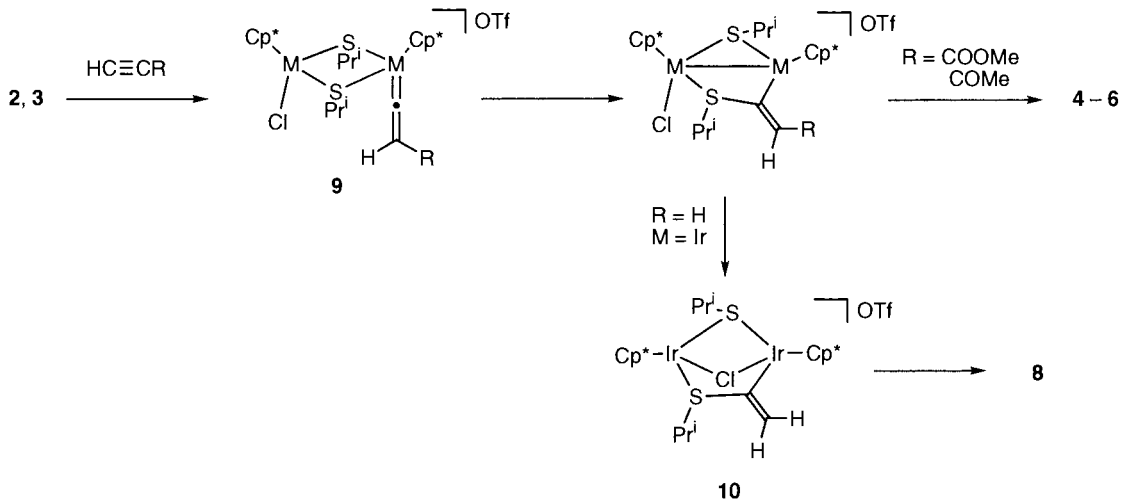

Scheme 1.

the chloro ligand and the change of the coordination mode of the α-(isopropylthio)vinyl ligand account for the formation of complex **8**. An intermediate with a μ-Cl ligand such as **10** is presumed to be involved in the isomerization process. It is very interesting to note that the reaction of the diruthenium complex **1** with acetylene gas, methyl propiolate, or 3-butyn-2-one yields the corresponding vinylidene complex that is stable enough to be isolated [5]. In contrast, the dirhodium and diiridium vinylidene complexes could not be obtained in the above reactions, and only complexes **4**–**6** and **8**, the products of the vinylidene–SPr^i coupling reaction, were isolated. Furthermore, as described above, monitoring the reaction of **2** and **3** with methyl propiolate by ^{1}H-NMR failed to detect the vinylidene intermediates. These facts strongly suggest that the vinylidene ligand at the dirhodium and diiridium centers is more susceptible to the intramolecular nucleophilic attack by the SPr^i ligand.

The reactions of complex **3** with 1,1-diphenyl- or 1,1-ditolyl-2-propyn-1-ol afforded the cationic (hydroxy)(vinyl)carbene complexes [Cp*IrCl(μ-SPr^i)$_2$-Ir{=C(OH)CH=CAr$_2$}Cp*][OTf] (**11**, Ar = Ph; **12**, Ar = Tol) (Eq. (4)), although no isolable product could be obtained from analogous reactions of complex **2**. Formation of complexes derived from the coupling of an SPr^i ligand and the alkyne molecule was not confirmed. Complex **11** exhibited doublets at δ 6.93 ($J = 2.0$ Hz) and 14.27 ($J = 2.0$ Hz) in its ^{1}H-NMR spectrum assignable to the vinyl and OH protons, respectively, as well as a ^{13}C{^{1}H}-NMR signal at δ 244.4 characteristic of a carbene ligand. These data agree well with the formulation. Similar spectral features were observed with complex **12**.

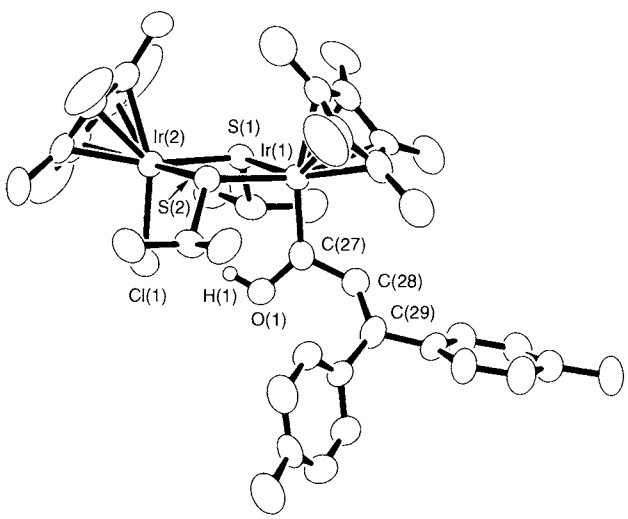

Fig. 4. Structure of the cationic part in **12**. Thermal ellipsoids are shown at the 50% probability level.

Table 4
Selected interatomic distances (Å) and angles (°) in **12**

Distances			
Ir(1)–S(1)	2.360(2)	Ir(1)–S(2)	2.379(2)
Ir(1)–C(27)	1.936(9)	Ir(2)–Cl(1)	2.412(2)
Ir(2)–S(1)	2.379(2)	Ir(2)–S(2)	2.390(2)
O(1)–C(27)	1.333(9)	C(27)–C(28)	1.46(1)
C(28)–C(29)	1.35(1)	Ir(1)···Ir(2)	3.6673(7)
Cl(1)···O(1)	2.986(5)	Cl(1)···H(1)	2.15
Angles			
S(1)–Ir(1)–S(2)	79.24(7)	S(1)–Ir(1)–C(27)	93.9(2)
S(2)–Ir(1)–C(27)	97.8(2)	Cl(1)–Ir(2)–S(1)	93.07(8)
Cl(1)–Ir(2)–S(2)	91.27(8)	S(1)–Ir(2)–S(2)	78.64(7)
Ir(1)–C(27)–O(1)	129.8(6)	Ir(1)–C(27)–C(28)	120.8(6)
O(1)–C(27)–C(28)	109.3(7)	C(27)–C(28)–C(29)	130.6(8)

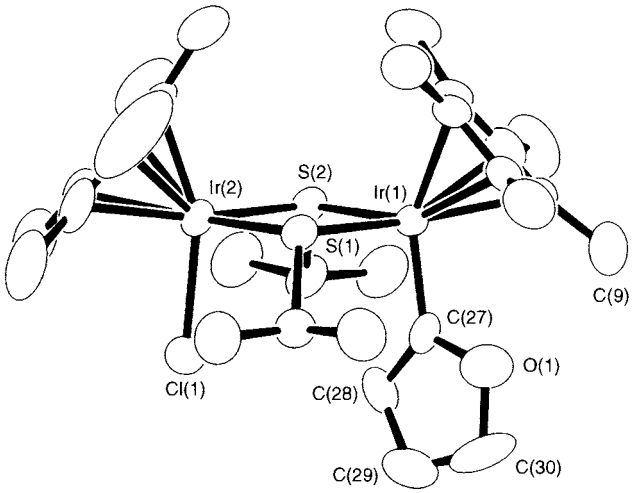

Fig. 5. Structure of the cationic part in **16**. Thermal ellipsoids are shown at the 50% probability level.

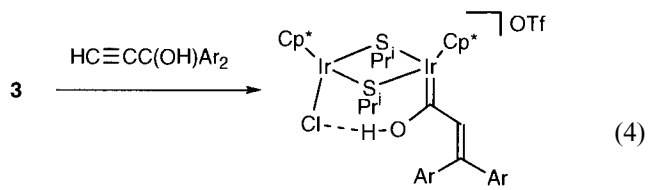

(4)

11: Ar= Ph
12: Ar = Tol

The molecular structure of **12** was determined by X-ray analysis. An ORTEP drawing for the cationic part in **12** is shown in Fig. 4, and selected bond distances and angles are summarized in Table 4. The Ir_2S_2 core is nearly planar, and the Ir(1) atom is confirmed to be bonded to the (hydroxy)(vinyl)carbene ligand. The short Ir(1)–C(27) and C(28)–C(29) distances at 1.936(9) and 1.35(1) Å, respectively, are congruent with the unsaturated carbene ligand. The hydroxy group on the carbene carbon forms an intramolecular hydrogen bond with the chloro ligand on the Ir(2) atom, where the Cl(1)···H(1) separation is estimated to be 2.15 Å. Hydroxycarbene complexes are usually unstable and easily converted into the corresponding acyl complexes by deprotonation [17,18]. The thermal stability of complexes **11** and **12** is most probably attributable to the intramolecular hydrogen bond involving the OH group. It is reasonable to consider that the formation of **11** and **12** is initiated with the dehydration of the propargylic alcohol at the cationic diiridium center to provide the dinuclear allenylidene species [Cp*IrCl(μ-SPr^i)$_2$Ir(=C=C=CAr_2)Cp*][OTf] (**13**) [19]. In general, the C_α and C_γ atoms of an allenylidene ligand are known to be susceptible to nucleophilic attack [20,21]. In the present case, nucleophilic attack of H_2O molecule at the C_α atom of the allenylidene ligand is considered to afford the (hydroxy)(vinyl)carbene derivatives **11** and **12**, although examples of such conversions of alkynols to (hydroxy)(vinyl)carbene ligands on metal centers have been limited in number [20].

Table 5
Selected interatomic distances (Å) and angles (°) in **16**

Distances			
Ir(1)–S(1)	2.381(2)	Ir(1)–S(2)	2.395(2)
Ir(1)–C(27)	1.949(7)	Ir(2)–Cl(1)	2.401(2)
Ir(2)–S(1)	2.380(2)	Ir(2)–S(2)	2.385(2)
O(1)–C(27)	1.352(9)	Ir(1)···Ir(2)	3.6901(4)
Angles			
S(1)–Ir(1)–S(2)	78.56(6)	S(1)–Ir(1)–C(27)	93.1(2)
S(2)–Ir(1)–C(27)	98.7(2)	Cl(1)–Ir(2)–S(1)	94.30(7)
Cl(1)–Ir(2)–S(2)	93.26(6)	S(1)–Ir(2)–S(2)	78.76(6)
Ir(1)–C(27)–O(1)	118.8(5)	Ir(1)–C(27)–C(28)	132.3(6)
O(1)–C(27)–C(28)	108.9(7)		

We previously reported that the diruthenium complex **1** reacts with 1,1-diaryl-2-propyn-1-ols to give the allenylidene complexes [Cp*RuCl(μ-SPr^i)$_2$Ru(=C=C=CAr_2)Cp*][OTf] (**14**) [3]. However, complex **14** failed to react with nucleophiles including H_2O at ambient temperature. This makes a sharp contrast to the above reaction of the diiridium analog **3**, where the facile addition of H_2O takes place, and the allenylidene species **13** is not isolated. The allenylidene ligand on the diiridium center is presumed to be more reactive toward nucleophiles than that on the diruthenium core.

Finally, reactions of complexes **2** and **3** with 3-butyn-1-ol and 4-pentyn-1-ol were examined. In each case, the dinuclear complex with a cyclic alkoxycarbene ligand [Cp*MCl(μ-SPr^i)$_2$M{=C$(CH_2)_{n+2}$O}Cp*][OTf] (**15**, M = Rh, $n = 1$; **16**, M = Ir, $n = 1$; **17**, M = Ir, $n = 2$) was obtained (Eq. (5)). In contrast to the reactions with other alkynes, the corresponding diruthenium complex [Cp*RuCl(μ-SPr^i)$_2$Ru{=C$(CH_2)_3$O}Cp*][OTf] (**18**) could also be isolated from the reaction of **1** with 3-butyn-1-ol. The formation of the cyclic carbene ligands is regarded to proceed via the initial formation of a vinylidene species and the succeeding nucleophilic attack of the ω-OH group at the vinylidene C_α atom [15].

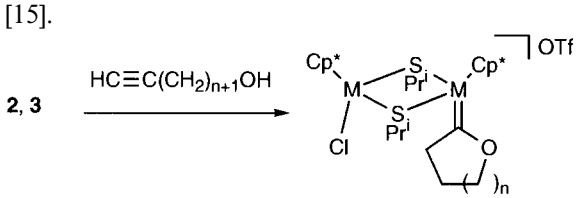

(5)

15: M = Rh, n = 1
16: M = Ir, n = 1
17: M = Ir, n = 2

The ^{1}H-NMR spectra of **15**–**17** displayed a set of signals due to the methylene protons of the cyclic carbene ligands. In addition, the $^{13}C\{^1H\}$-NMR spectrum of **16** exhibited a low field signal at δ 267.2 diagnostic of a carbene carbon. The molecular structure of **16** was further confirmed crystallographically. As shown in Fig. 5, complex **16** is composed of an Ir_2S_2

core closely related to that of **12** and a cyclic carbene ligand which is almost planar and twisted from the Ir(2)–Ir(1)–C(27) plane with the dihedral angle of 28.4°. This conformation is probably due to the steric congestion between the carbene ring and the Cp* ligand on the Ir(1) atom. In fact, the O(1) atom in the carbene ligand is located considerably close to one of the Cp* Me groups (C(9)) with the O(1)···C(9) distance of 2.95 Å (Table 5).

2.3. Molecular orbital calculations for model vinylidene complexes

As described above, terminal alkynes are readily converted into α-(isopropylthio)vinyl, (hydroxy)(vinyl)-carbene, or cyclic alkoxycarbene ligands at the cationic dirhodium and diiridium centers of **2** and **3** by way of the vinylidene or allenylidene species. Interestingly, these vinylidene and allenylidene species seem to possess higher reactivities in nucleophilic addition reactions than the diruthenium analogs. Since the set of auxiliary ligands and the net charge of the dinuclear cores in these systems are the same, it is presumed that the electronic structures of the cores affect the reactivities of the vinylidene and allenylidene ligands. Indeed, the dirhodium or diiridium and diruthenium systems differ in their numbers of valence electrons in the dinuclear cores. The former is expected to have a 36 e^- core without a metal–metal bond, while the latter has a 34 e^- core with a metal–metal bonding interaction [3,5]. In order to obtain insight into their electronic structures, extended Hückel molecular orbital (EHMO) calculations were performed for the hypothetical C_s-idealized dinuclear vinylidene complexes $[CpMCl(\mu\text{-}SH)_2M(=C=CH_2)Cp]^+$ (**19**, M = Ru; **20**, M = Ir; Cp = η^5-C_5H_5) which were modeled from the crystallographically determined complexes $[Cp^*RuCl(\mu\text{-}SPr^i)_2Ru(=C=CHCOOMe)Cp^*][OTf]$ (**21**) [5] and **16**, respectively.

Kostić and Fenske claimed that the addition of a nucleophile at the C_α atom of a vinylidene ligand is frontier orbital-controlled, and the reactivity is related to the characteristics that the LUMO is (1) π antibonding between the M–C_α bond, (2) localized at the C_α atom, and (3) separated in energy from the LUMO + 1 [22]. Chart 1 depicts the LUMOs obtained for **19** and **20** in which the M=C=CH_2 plane is oriented perpendicular to the mirror plane of the cation. The LUMO of the diruthenium model complex **19** is a Ru–Ru antibonding orbital, and the atomic orbitals of the C_α atom of the vinylidene ligand have essentially no contribution to the LUMO. Thus, the vinylidene ligand in **19** is not the primary reaction center in the orbital-controlled nucleophilic additions, since the LUMO does not satisfy the above criteria. This result clearly corresponds to the fact that diruthenium vinylidene complexes such as **21** are stable and isolable compounds. The exceptional reaction leading to complex **18** may be ascribed to the kinetically favored five-membered ring formation.

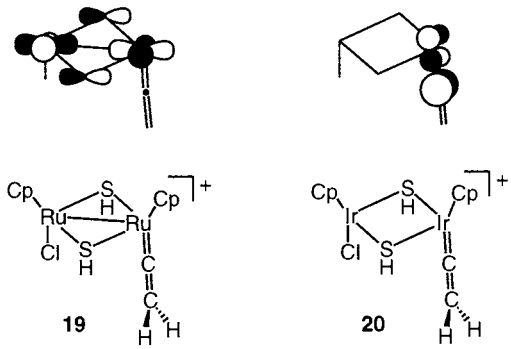

(Chart 1)

In contrast, the LUMO of the diiridium species **20** is π antibonding with respect to the Ir–C_α bond and is strongly localized at these atoms. A relatively large energy difference (0.9 eV) was observed between the LUMO and LUMO + 1. Obviously the LUMO of **20** fulfills the above-mentioned criteria to make the vinylidene C_α atom reactive in nucleophilic additions, and therefore, the vinylidene ligand in the diiridium (and also dirhodium) complex **9** is expected to be susceptible to nucleophilic attack of an SPr^i ligand. This is the reason why complex **9** could not be isolated. We also consider that the reactivities of allenylidene ligands in **13** and **14** are controlled similarly, but it is not clear why the allenylidene ligand in **13** undergoes the reaction with H_2O rather than the coupling with an SPr^i ligand. Molecular orbital calculations were also performed for models with the vinylidene ligand coplanar to the M–M axis, but important features found for the LUMOs are essentially the same as those shown in Chart 1. These calculation results are fully consistent with the observed differences in the reactivities between the diiridium (or dirhodium) and diruthenium systems. In the EHMO calculations, however, the energy levels are qualitative, and calculations of higher level are needed for more detailed discussions.

In conclusion, we have demonstrated that the cationic dinuclear dirhodium and diiridium complexes **2** and **3** readily incorporate one terminal alkyne molecule to form a series of complexes with vinyl or carbene ligands, and the high reactivities of the intermediate vinylidene species are interpreted on the basis of the molecular orbital calculations. These results provide an interesting example in which it is shown experimentally as well as theoretically that the valence electron numbers of the dinuclear cores directly influence the reactivities of the vinylidene type ligands.

3. Experimental

3.1. General considerations

All manipulations were performed using standard Schlenk tube techniques. Complexes **1** [3], **2**, and **3** [7]

were prepared according to the procedure previously described. 1,1-Diphenyl-2-propyn-1-ol and 1,1-ditolyl-2-propyn-1-ol were prepared as described in the literature [23]. Solvents were dried and distilled prior to use. Other reagents were commercially obtained and used without further purification. IR spectra were recorded on a Shimadzu 8100M spectrometer. ^{1}H- (270 MHz) and ^{13}C{^{1}H}-(67.8 MHz)NMR spectra were obtained on a JEOL EX-270 spectrometer. Elemental analyses were performed on a Perkin–Elmer 2400II CHN analyzer.

3.2. Preparation of [Cp*RhCl(μ-SPr^i)-{μ-S(Pr^i)C=CHCOOMe}RhCp*][OTf] (4)

To a solution of **2** (132 mg, 0.162 mmol) in acetone (5 ml) was added methyl propiolate (60 mg, 0.83 mmol), and the mixture was stirred at room temperature for 2 h. Longer reaction time caused precipitation of uncharacterized byproducts. The solvent was removed in vacuo, and the residue was dissolved in acetone. Addition of ether to the filtered acetone solution gave **4** as orange–red crystals (98 mg, 0.109 mmol, 68%). IR (cm^{-1}): 1572 [ν(C=O)]. ^{1}H-NMR ($CDCl_3$): δ 1.08, 1.15, 1.47, 1.51 (d, 3H each, $J = 6.6$ Hz, SCHMe_2), 1.59, 1.64 (s, 15H each, Cp*), 1.87, 4.00 (sep, 1H each, $J = 6.6$ Hz, SCHMe$_2$), 3.76 (s, 3H, COOMe), 6.18 (s, 1H, vinyl). Anal. Calc. for $C_{31}H_{48}ClF_3O_5Rh_2S_3$: C, 41.59; H, 5.40. Found: C, 41.55; H, 5.48%.

3.3. Preparation of [Cp*IrCl(μ-SPr^i){μ-S(Pr^i)C=CHCOOMe}IrCp*][OTf] (5)

To a solution of **3** (118 mg, 0.119 mmol) in CH_2Cl_2 (5 ml) was added methyl propiolate (51 mg, 0.60 mmol), and the mixture was stirred at r.t. for 24 h. The orange solution was evaporated to dryness, and the residue was dissolved in acetone. Addition of ether to the filtered acetone solution gave **5** as dark orange crystals (99 mg, 0.092 mmol, 78%). IR (cm^{-1}): 1559 [ν(C=O)]. ^{1}H-NMR (acetone–d_6): δ 1.07, 1.20, 1.49, 1.62 (d, 3H each, $J =$ 6.6 Hz, SCHMe_2), 1.71, 1.74 (s, 15H each, Cp*), 2.12, 4.13 (sep, 1H each, $J = 6.6$ Hz, SCHMe$_2$), 3.96 (s, 3H, COOMe), 7.15 (s, 1H, vinyl). Anal. Calc. for $C_{31}H_{48}ClF_3Ir_2O_5S_3$: C, 34.67; H, 4.51. Found: C, 34.71; H, 4.54%.

3.4. Preparation of [Cp*IrCl(μ-SPr^i){μ-S(Pr^i)-C=CHCOMe}IrCp*][OTf] (6)

To a solution of **3** (105 mg, 0.106 mmol) in CH_2Cl_2 (5 ml) was added 3-butyn-2-one (37 mg, 0.54 mmol), and the mixture was stirred at r.t. for 24 h. The orange solution was evaporated to dryness, and the residue was dissolved in acetone. Addition of ether to the filtered acetone solution gave **6** as dark orange crystals (90 mg, 0.085 mmol, 80%). IR (cm^{-1}): 1541 [ν(C=O)]. ^{1}H-NMR (acetone-d_6): δ 1.02, 1.15, 1.48, 1.61 (d, 1H each, $J = 6.6$ Hz, SCHMe_2), 1.69, 1.76 (s, 15H each, Cp*), 1.98, 4.20 (sep, 1H each, $J = 6.6$ Hz, SCHMe$_2$), 2.51 (s, 3H, COMe), 7.69 (s, 1H, vinyl). Anal. Calc. for $C_{31}H_{48}ClF_3Ir_2O_4S_3$: C, 35.20; H, 4.57. Found: C, 35.56; H, 4.70%.

3.5. Preparation of [Cp*IrCl(μ-SPr^i){μ-C(SPr^i)=CH$_2$}IrCp*][OTf] (8)

Acetylene gas was bubbled through a solution of complex **3** (132 mg, 0.138 mmol) in acetone (5 ml) for 5 min. The color of the solution immediately changed from orange to red–purple. The solution was stirred at r.t. for 24 h, and the solvent was removed in vacuo. The residue was dissolved in THF, and ether was added to the THF solution to give **8** as red–purple crystals (74 mg, 0.073 mmol, 53%). ^{1}H-NMR ($CDCl_3$): δ 1.23, 1.44 (d, 3H each, $J = 6.6$ Hz, SCHMe_2), 1.34 (d, 6H, $J = 6.6$ Hz, SCHMe_2), 1.85, 1.91 (s, 15H each, Cp*), 3.41 (d, 1H, $J = 3.5$ Hz, vinyl), 3.63, 3.70 (sep, 1H each, $J = 6.6$ Hz, SCHMe$_2$), 4.47 (d, 1H, $J = 3.5$ Hz, vinyl). Anal. Calc. for $C_{29}H_{46}ClF_3Ir_2O_3S_3$: C, 34.29; H, 4.56. Found: C, 34.27; H, 4.65%. The corresponding $[PF_6]^-$ salt [Cp*IrCl(μ-SPr^i){μ-C(SPr^i)=CH$_2$}IrCp*][PF_6]·THF (**8′**·THF), which was used for crystallographic study, was obtained as red–purple crystals by anion metathesis of **8** with KPF_6 in acetone and recrystallization from THF–ether.

3.6. Preparation of [Cp*IrCl(μ-SPr^i)$_2$Ir{=C(OH)CH=CPh$_2$}Cp*][OTf] (11)

To a solution of **3** (108 mg, 0.109 mmol) in CH_2Cl_2 (5 ml) was added 1,1-diphenyl-2-propyn-1-ol (116 mg, 0.56 mmol), and the mixture was stirred at r.t. for 24 h. During this period, the color of the solution changed from yellow to wine red. The resulting mixture was evaporated in vacuo, and the residue was washed three times with ether (3 ml) and dissolved in acetone. Addition of ether to the acetone solution gave **11** as purple–brown crystals (54 mg, 0.045 mmol, 41%). ^{1}H-NMR (acetone-d_6): δ 1.01, 1.07 (d, 6H each, $J = 6.6$ Hz, SCHMe_2), 1.62, 1.80 (s, 15H each, Cp*), 2.74 (sep, 2H, $J = 6.6$ Hz, SCHMe$_2$), 6.93 (d, 1H, $J = 2.0$ Hz, vinyl), 7.21–7.24 (m, 2H, Ph), 7.41–7.47 (m, 8H, Ph), 14.27 (d, 1H, $J = 2.0$ Hz, OH); ^{13}C{^{1}H}-NMR ($CDCl_3$): δ 8.7, 9.2, 20.8, 22.4, 32.0, 92.1, 102.3, 127.9, 128.4, 128.7, 128.9, 129.1, 130.4, 139.3, 139.6, 140.8, 151.3, 244.4. Anal. Calc. for $C_{42}H_{56}ClF_3Ir_2O_4S_3$: C, 42.11; H, 4.71. Found: C, 42.41; H, 4.79%.

3.7. Preparation of [Cp*IrCl(μ-SPr^i)$_2$Ir{=C(OH)-CH=CTol$_2$}Cp*][OTf] (12)

To a solution of **3** (132 mg, 0.134 mmol) in CH_2Cl_2 (5 ml) was added 1,1-ditolyl-2-propyn-1-ol (200 mg, 0.85

mmol), and the mixture was stirred at r.t. for 24 h. During this period, the color of the solution changed from yellow to red–brown. The resulting mixture was evaporated in vacuo, and the residue was washed three times with ether (3 ml) and dissolved in CH_2Cl_2. Addition of ether to the CH_2Cl_2 solution gave **12** as orange needles (98 mg, 0.080 mmol, 59%). ^{1}H-NMR (acetone-d_6): δ 1.03, 1.08 (d, 6H each, $J = 6.7$ Hz, SCHMe_2), 1.62, 1.79 (s, 15H each, Cp*), 2.34, 2.39 (s, 3H each, C_6H_4Me), 2.78 (sep, 2H, $J = 6.7$ Hz, SCHMe$_2$), 6.85 (d, 1H, $J = 1.8$ Hz, vinyl), 7.05 (d, 2H, $J = 7.9$ Hz, aryl), 7.18–7.28 (m, 6H, aryl), 14.12 (d, 1H, $J = 1.8$ Hz, OH); ^{13}C{^{1}H}-NMR ($CDCl_3$): δ 8.7, 9.1, 20.8, 21.4, 22.4, 31.9, 92.0, 102.0, 128.5, 128.6, 128.9, 129.7, 136.5, 138.5, 138.7, 139.1, 141.0, 152.4, 243.6. Anal. Calc. for $C_{44}H_{60}ClF_3Ir_2O_4S_3$: C, 43.10; H, 4.93. Found: C, 42.81; H, 4.96%.

3.8. Preparation of [Cp*RhCl(μ-SPr^i)$_2$Rh{=C(CH$_2$)$_3$O}-Cp*][OTf] (15)

To a solution of **2** (115 mg, 0.142 mmol) in acetone (5 ml) was added 3-butyn-1-ol (51 mg, 0.73 mmol), and the mixture was stirred at r.t. for 24 h. The solvent was removed in vacuo, and the residue was dissolved in acetone. Addition of ether to the filtered acetone solution gave **15** as orange–red crystals (77 mg, 0.087 mmol, 61%). ^{1}H-NMR ($CDCl_3$): δ 0.91, 1.10 (d, 6H each, $J =$ 6.6 Hz, SCHMe_2), 1.55, 1.64 (s, 15H each, Cp*), 2.18 (quint, 2H, $J = 7.6$ Hz, $CH_2CH_2CH_2$), 2.86 (sep, 2H, $J = 6.6$ Hz, SCHMe$_2$), 4.16 (t, 2H, $J = 7.6$ Hz, =CCH_2), 5.25 (t, 2H, $J = 7.6$ Hz, OCH_2). Anal. Calc. for $C_{31}H_{50}ClF_3O_4Rh_2S_3$: C, 42.25; H, 5.72. Found: C, 42.59; H, 5.84%.

3.9. Preparation of [Cp*IrCl(μ-SPr^i)$_2$Ir{=C(CH$_2$)$_3$O}-Cp*][OTf] (16)

To a solution of **3** (128 mg, 0.129 mmol) in CH_2Cl_2 (5 ml) was added 3-butyn-1-ol (46 mg, 0.65 mmol), and the mixture was stirred at r.t. for 24 h to give a yellow solution. The solvent was removed in vacuo, and the residue was dissolved in CH_2Cl_2. Addition of ether to the CH_2Cl_2 solution gave **16** as yellow crystals (126 mg, 0.119 mmol, 92%). ^{1}H-NMR (acetone-d_6): δ 0.86, 1.04 (d, 6H each, $J = 6.6$ Hz, SCHMe_2), 1.59, 1.78 (s, 15H each, Cp*), 2.26 (quint, 2H, $J = 7.6$ Hz, $CH_2CH_2CH_2$), 3.15 (sep, 2H, $J = 6.6$ Hz, SCHMe$_2$), 3.57 (t, 2H, $J = 7.6$ Hz, =CCH_2), 5.14 (t, 2H, $J = 7.6$ Hz, OCH_2); ^{13}C{^{1}H}-NMR (acetone-d_6): δ 9.1, 9.7, 22.1, 23.0, 23.8, 33.9, 59.9, 86.0, 92.6, 102.0, 262.9. Anal. Calc. for $C_{31}H_{50}ClF_3Ir_2O_4S_3$: C, 35.13; H, 4.76. Found: C, 35.28; H, 4.78%.

3.10. Preparation of [Cp*IrCl(μ-SPr^i)$_2$Ir{=C(CH$_2$)$_4$O}-Cp*][OTf] (17)

To a solution of **3** (122 mg, 0.123 mmol) in CH_2Cl_2 (5 ml) was added 4-pentyn-1-ol (53 mg, 0.63 mmol), and the mixture was stirred at r.t. for 24 h. The resulting yellow solution was evaporated in vacuo, and the residue was dissolved in CH_2Cl_2. Addition of ether to the CH_2Cl_2 solution gave **17** as yellow crystals (79 mg, 0.074 mmol, 60%). ^{1}H-NMR (acetone-d_6): δ 0.90, 1.05 (d, 6H each, $J = 6.6$ Hz, SCHMe_2), 1.59, 1.76 (s, 15H each, Cp*), 1.93, 2.11 (m, 2H each, $CH_2CH_2CH_2$), 3.12 (sep, 2H, $J = 6.6$ Hz, SCHMe$_2$), 3.33 (t, 2H, $J = 6.8$ Hz, =CCH_2), 4.97 (t, 2H, $J = 5.9$ Hz, OCH_2). Anal. Calc. for $C_{32}H_{52}ClF_3Ir_2O_4S_3$: C, 35.79; H, 4.88. Found: C, 35.87; H, 4.90%.

3.11. Preparation of [Cp*RuCl(μ-SPr^i)$_2$Ru{=C(CH$_2$)$_3$O}Cp*][OTf] (18)

To a solution of **1** (128 mg, 0.155 mmol) in CH_2Cl_2 (5 ml) was added 3-butyn-1-ol (56 mg, 0.79 mmol), and the mixture was stirred at r.t. for 24 h. The resulting solution was evaporated in vacuo, and the residue was dissolved in CH_2Cl_2. Addition of hexane to the CH_2Cl_2 solution gave **18** as dark brown crystals (119 mg, 0.136 mmol, 87%). ^{1}H-NMR ($CDCl_3$): δ 1.43, 1.69 (d, 6H each, $J =$ 6.6 Hz, SCHMe_2), 1.60, 1.68 (s, 15H each, Cp*), 1.87 (quint, 2H, $J = 7.5$ Hz, $CH_2CH_2CH_2$), 3.25 (t, 2H, $J =$ 7.5 Hz, =CCH_2), 3.93 (sep, 2H, $J = 6.6$ Hz, SCHMe$_2$), 4.80 (t, 2H, $J = 7.5$ Hz, OCH_2). Anal. Calc. for $C_{31}H_{50}ClF_3O_4Ru_2S_3$: C, 42.43; H, 5.74. Found: C, 42.37; H, 5.90%.

3.12. X-ray crystallographic studies

Single crystals of **3**, **4**, **5**, **8′**·THF, **12**, and **16** were sealed in glass capillaries under an argon atmosphere and used for data collection. Diffraction data were collected on a Rigaku AFC7R four-circle automated diffractometer with graphite-monochromatized Mo–K_α radiation ($\lambda = 0.71069$ Å) at 294 K using the ω–2θ scan technique for **3**, **4**, **5**, **8′**·THF, and **16** and the ω-scan technique for **12** ($5° < 2\theta < 55°$ for **3**, **4**, **5**, **8′**·THF, and **12**; $5° < 2\theta < 50°$ for **16**). Intensity data were corrected for Lorentz and polarization effects and for absorption (empirical, ψ scans). For crystals of **3**, **4**, **5**, **12**, and **16**, no significant decay was observed for three standard reflections monitored every 150 reflections during the data collection. For compound **8′**·THF, slight decay (2.28%) was observed during the data collection, and a correction for decay was applied.

The structure solution and refinements were carried out by using the teXsan crystallographic software package [24]. The positions of the non-hydrogen atoms were determined by Patterson methods (DIRDIF PATTY [25]) and subsequent Fourier syntheses. All non-hydrogen atoms were refined by full-matrix least-squares techniques (based on F) with anisotropic thermal parameters except for the carbon, oxygen, and fluorine atoms of $[OTf]^-$ anion in **12**, where isotropic thermal parameters

were used. The oxygen and fluorine atoms of the $[OTf]^-$ anion in **12** were found to be disordered, and each of these atoms was placed at two positions and refined with the occupancies of 0.6 and 0.4. The hydrogen atom of the OH group in **12** was found in the final difference Fourier map, while the other hydrogen atoms were placed at the calculated positions (d_{C-H} = 0.95 Å). These hydrogen atoms were included in the final stage of refinements with fixed isotropic parameters. Details of the X-ray diffraction study are summarized in Tables 6 and 7.

3.13. Molecular orbital calculations

All molecular orbital calculations were performed on CAChe system by employing the extended Hückel method with the parameters taken from the literature [26], where 3*d* orbitals of the sulfur atoms were not included in the calculations. The non-hydrogen atoms in **19** and **20** were placed according to C_s-idealized structures where the M=C=CH_2 plane is oriented perpendicular or parallel to the mirror plane of the cation; they are based on the observed structures of **21** [5] and **16**, respectively.

Table 6
X-ray crystallographic data for **3**, **4**, and **5**

	3	**4**	**5**
Formula	$C_{27}H_{44}ClF_3Ir_2O_3S_3$	$C_{31}H_{48}ClF_3O_5Rh_2S_3$	$C_{31}H_{48}ClF_3Ir_2O_5S_3$
Formula weight	989.71	895.16	1073.79
Crystal system	Monoclinic	Monoclinic	Monoclinic
Space group	$P2_1/c$	$P2_1/n$	$P2_1/a$
Crystal size (mm)	0.25 × 0.30 × 0.40	0.20 × 0.35 × 0.40	0.20 × 0.40 × 0.55
a (Å)	11.057(2)	19.560(2)	19.537(2)
b (Å)	13.654(2)	22.422(2)	22.383(3)
c (Å)	22.345(3)	8.787(2)	8.829(2)
β (°)	100.87(1)	103.13(1)	102.82(1)
V (Å^3)	3313.0(9)	3753.0(8)	3764(1)
Z	4	4	4
μ(Mo–K_α) (cm^{-1})	83.61	11.66	73.69
Unique reflections	7602 (R_{int} = 0.032)	8633 (R_{int} = 0.025)	8661 (R_{int} = 0.045)
Observed reflections	4281 ($I > 3\sigma(I)$)	5040 ($I > 3\sigma(I)$)	5441 ($I > 3\sigma(I)$)
R [a]	0.038	0.041	0.049
R_w [b]	0.031	0.029	0.029
Goodness-of-fit [c]	1.65	1.62	2.07

[a] $R = \Sigma||F_o| - |F_c||/\Sigma|F_o|$.
[b] $R_w = [\Sigma w(|F_o| - |F_c|)^2/\Sigma wF_o^2]^{1/2}$, $w = 1/\sigma^2(F_o)$.
[c] GOF = $[\Sigma w(|F_o| - |F_c|)^2/(N_{obs} - N_{params})]^{1/2}$.

Table 7
X-ray crystallographic data for **8′**·THF, **12**, and **16**

	8′·THF	**12**	**16**
Formula	$C_{32}H_{54}ClF_6Ir_2OPS_2$	$C_{44}H_{60}ClF_3Ir_2O_4S_3$	$C_{31}H_{50}ClF_3Ir_2O_4S_3$
Formula weight	1083.76	1226.02	1059.80
Crystal system	Monoclinic	Monoclinic	Triclinic
Space group	$P2_1/c$	$P2_1/n$	$P\bar{1}$
Crystal size (mm)	0.20 × 0.20 × 0.65	0.10 × 0.30 × 0.60	0.15 × 0.40 × 0.70
a (Å)	14.705(2)	12.038(3)	9.680(2)
b (Å)	12.390(3)	15.313(2)	13.328(4)
c (Å)	21.250(2)	25.735(2)	15.378(3)
α (°)			72.48(2)
β (°)	94.62(1)	101.173(9)	78.27(2)
γ (°)			84.55(2)
V (Å^3)	3858.9(9)	4653(1)	1851.2(8)
Z	4	4	2
μ (Mo–K_α) (cm^{-1})	71.81	59.72	74.90
Unique reflections	8834 (R_{int} = 0.054)	10683 (R_{int} = 0.041)	6521 (R_{int} = 0.035)
Observed reflections	4905 ($I > 3\sigma(I)$)	6349 ($I > 3\sigma(I)$)	5098 ($I > 3\sigma(I)$)
R [a]	0.050	0.041	0.031
R_w [b]	0.036	0.031	0.029
Goodness-of-fit [c]	1.81	1.36	2.25

[a] $R = \Sigma||F_o| - |F_c||/\Sigma|F_o|$.
[b] $R_w = [\Sigma w(|F_o| - |F_c|)^2/\Sigma wF_o^2]^{1/2}$, $w = 1/\sigma^2(F_o)$.
[c] GOF = $[\Sigma w(|F_o| - |F_c|)^2/(N_{obs} - N_{params})]^{1/2}$.

4. Supplementary material

Crystallographic data for the structural analysis have been deposited with the Cambridge Crystallographic Data Centre, CCDC nos. 136329 (compound **3**), 136330 (compound **4**), 136331 (compound **5**), 136332 (compound **8′**·THF), 136333 (compound **12**), and 136334 (compound **16**). Copies of this information may be obtained free of charge from The Director, CCDC, 12 Union Road, Cambridge, CB2 1EZ, UK (Fax. + 44-1223-336-033, or E-mail: deposit@ccdc.cam.ac.uk or www:http://www.ccdc.cam.ac.uk).

Acknowledgements

This work was supported by a Grant-in-aid for Specially Promoted Research (09102004) from the Ministry of Education, Science, Sports, and Culture, Japan.

References

[1] (a) R.D. Adams, F.A. Cotton (Eds.), Catalysis by Di- and Polynuclear Metal Cluster Complexes, Wiley–VCH, New York, 1998. (b) G. Süss-Fink, G. Meister, Adv. Organomet. Chem. 35 (1993) 41.

[2] (a) M. Hidai, Y. Mizobe, H. Matsuzaka, J. Organomet. Chem. 473 (1994) 1. (b) M. Hidai, Y. Mizobe, in: E.I. Stiefel, K. Matsumoto (Eds.), Transition Metal Sulfur Chemistry: Biological and Industrial Significance, ACS Symposium Series 653, American Chemical Society: Washington, DC, 1996, p. 310. (c) M. Hidai, S. Kuwata, Y. Mizobe, Acc. Chem. Res. 33 (2000) 46.
[3] H. Matsuzaka, Y. Takagi, M. Hidai, Organometallics 13 (1994) 13.
[4] H. Matsuzaka, Y. Takagi, Y. Ishii, M. Nishio, M. Hidai, Organometallics 14 (1995) 2153.
[5] Y. Takagi, H. Matsuzaka, Y. Ishii, M. Hidai, Organometallics 16 (1997) 4445.
[6] J.-P. Qü, D. Masui, Y. Ishii, M. Hidai, Chem. Lett. (1998) 1003.
[7] T. Iwasa, H. Shimada, A. Takami, H. Matsuzaka, Y. Ishii, M. Hidai, Inorg. Chem. 38 (1999) 2851.
[8] M. Nishio, H. Matsuzaka, Y. Mizobe, M. Hidai, Inorg. Chim. Acta 263 (1997) 119.
[9] M. Nishio, Y. Mizobe, H. Matsuzaka, M. Hidai, Inorg. Chim. Acta 265 (1997) 59.
[10] H. Matsuzaka, J.-P. Qü, T. Ogino, M. Nishio, Y. Nishibayashi, Y. Ishii, S. Uemura, M. Hidai, J. Chem. Soc. Dalton Trans. (1996) 4307.
[11] (a) T.B. Marder, D.M.-T. Chan, W.C. Fultz, D. Milstein, J. Chem. Soc. Chem. Commun. (1988) 996. (b) W.D. Jones, V.L. Chandler, F.J. Feher, Organometallics 9 (1990) 164.
[12] G.J. Sunley, P.d.C. Menanteau, H. Adams, N.A. Bailey, P.M. Maitlis, J. Chem. Soc. Dalton Trans. (1989) 2415.
[13] P.D. Morran, R.J. Mawby, G.D. Wilson, M.H. Moore, Chem. Commun. (Cambridge) (1996) 261.
[14] (a) A.M. Mueting, P.D. Boyle, R. Wagner, L.H. Pignolet, Inorg. Chem. 27 (1988) 271. (b) F.A. Cotton, P. Lahuerta, J. Latorre, M. Sanaú, I. Solana, W. Schwotzer, Inorg. Chem. 27 (1988) 2131. (c) W.D. Jones, R.M. Chin, J. Am. Chem. Soc. 116 (1994) 198. (d) D.A. Vicic, W.D. Jones, Organometallics 16 (1997) 1912. (e) Z. Tang, Y. Nomura, S. Kuwata, Y. Ishii, Y. Mizobe, M. Hidai, Inorg. Chem. 37 (1998) 4909.
[15] (a) M.I. Bruce, A.G. Seincer, Adv. Organomet. Chem. 22 (1983) 59. (b) S.G. Davies, J.P. McNally, A.J. Smallridge, Adv. Organomet. Chem. 30 (1990) 1. (c) M.I. Bruce, Chem. Rev. 91 (1991) 197.
[16] C. Bianchini, D. Masi, A. Romerosa, F. Zanobini, M. Peruzzini, Organometallics 18 (1999) 2376.
[17] C. Bianchini, J.A. Casares, M. Peruzzini, A. Romerosa, F. Zanobini, J. Am. Chem. Soc. 118 (1996) 4585.
[18] C. Bianchini, A. Marchi, L. Marveli, M. Peruzzini, A. Romerosa, R. Rossi, Organometallics 15 (1996) 3804.
[19] J.P. Selegue, Organometallics 1 (1982) 217.
[20] M.A. Esteruelas, A.V. Gómez, F.J. Lahoz, A.M. López, E. Oñate, L.A. Oro, Organometallics 15 (1996) 3423.
[21] (a) R. Le Lagadec, E. Roman, L. Toupet, U. Müller, P.H. Dixneuf, Organometallics 13 (1994) 5030. (b) V. Cadierno, M.P. Gamasa, J. Gimeno, M.C. López-González, J. Borge, S. García-Granda, Organometallics 16 (1997) 4453. (c) M.A. Esteruelas, A.V. Gómez, A.M. López, J. Modrego, E. Oñate, Organometallics 16 (1997) 5826. (d) C. Bianchini, M. Peruzzini, F. Zanobini, C. Lopez, I. de los Rios, A. Romerosa, Chem. Commun. (Cambridge) (1999) 443.
[22] N.M. Kostić, R.F. Fenske, Organometallics 1 (1982) 974.
[23] M.M. Midland, J. Org. Chem. 40 (1975) 2250.
[24] teXsan: Crystal Structure Analysis Package Molecular Structure Corp., The Woodlands, TX, 1985 and 1992.
[25] PATTY: P.T. Beurskens, G. Admiraal, G. Beurskens, W.P. Bosman, S. Garcia-Granda, R.O. Gould, J.M.M. Smits, C. Smykalla, The DIRDIF program system Technical Report of the Crystallography Laboratory, University of Nijmegen: Nijmegen, The Netherlands, 1992.
[26] (a) H. Berke, R. Hoffmann, J. Am. Chem. Soc. 100 (1978) 7224. (b) Y. Jiang, A. Tang, R. Hoffmann, J. Huang, J. Lu, Organometallics 4 (1985) 27. (c) A.R. Siedle, R.A. Newmark, L.H. Pignolet, D.X. Wang, T.A. Albright, Organometallics 5 (1986) 38.